

PROPER MOTIONS AND INTERNAL DYNAMICS IN THE CORE OF THE GLOBULAR CLUSTER M71

RAMINDER SINGH SAMRA<sup>1</sup>, HARVEY B. RICHER<sup>1</sup>, JEREMY S. HEYL<sup>1</sup>, RYAN GOLDSBURY<sup>1</sup>, KARUN THANJAVUR<sup>2</sup>, GORDON WALKER<sup>1</sup>, AND KRISTIN A. WOODLEY<sup>1</sup>

*Draft version July 31, 2018*

ABSTRACT

We have used Gemini North together with the NIRI-ALTAIR adaptive optics imager in the H and K bands to explore the core of the Galactic globular cluster M71 (NGC 6838). We obtained proper motions for 217 stars and have resolved its internal proper motion dispersion. Using a 3.8 year baseline, the proper motion dispersion in the core is found to be  $179 \pm 17 \mu\text{arcsec/yr}$ . We find no evidence of anisotropy in the motions and no radial variation in the proper motions with respect to distance from the cluster center. We also set an upper limit on any central black hole to be  $\sim 150 M_{\odot}$  at 90% confidence level.

*Subject headings:* astrometry — globular clusters: individual (M71, NGC 6838) — methods: data analysis — stars: kinematics and dynamics

1. INTRODUCTION

It has been recently shown that the cores of globular clusters (GCs) may be hosts of Intermediate Mass Black Holes (IMBHs), which have masses from  $\sim 100 M_{\odot}$  to several  $10^4 M_{\odot}$  (e.g. Noyola et al. 2008; Lützgendorf et al. 2011). If they are present, they could provide the missing link between supermassive black holes (SMBHs) in the cores of galaxies to stellar mass black holes (e.g. Maccarone et al. 2007).

IMBHs can be detected in several ways; a rise in the stellar density towards the cluster centre (Ibata et al. 2009), x-ray or radio emission (Ulvestad et al. 2007) or via a kinematic signature. Most GCs contain little gas therefore an IMBH would likely be most easily detected in the kinematics of its stars. Such signatures could be stars moving faster than the escape velocity of the cluster, a steep increase in the velocity dispersion profile towards the center, or observing orbital motion about the central BH, as seen in the center of the Galaxy (Ghez et al. 2005). N-body simulations (Baumgardt et al. 2005; Trenti et al. 2007) have suggested that clusters with large cores potentially harbour IMBHs, which provide an energy source to ‘fluff-up’ the central region of the cluster. Within this context, M71’s core radius is  $\sim 38''$  (Harris 2010) larger than  $\sim 70\%$  of all Galactic GCs.

An existing proper motion (hereafter PM) study was done by Cudworth (1985) where it was determined that M71 exhibits a low space velocity for a GC and that it was on a disk-like orbit in the Galaxy. Cudworth (1985) also calculated the PM dispersion for stars  $100''$  from the center and found it to be  $180 \pm 30 \mu\text{arcsec/yr}$ .

Modern values of the parameters describing M71 can be found in Harris (2010). The distance to M71 was determined several times, Arp & Hartwick (1971) place the cluster at  $4100 \pm 400\text{pc}$ , Geffert & Maintz (2000)

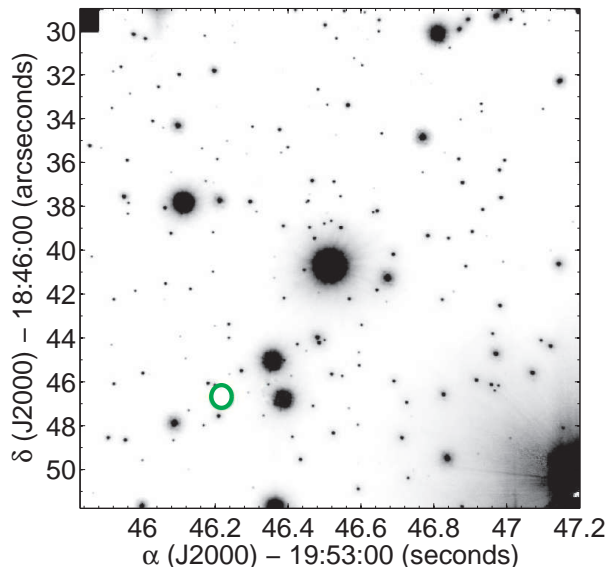


FIG. 1.— The core of M71 as imaged by the Gemini Telescope with the NIRI/ALTAIR AO system in H band. The telescope’s dither pattern resulted in a field that is 23.5 arcseconds on each side. The center of the small circle indicates the cluster center from Goldsbury et al. (2010) with a  $\sim 0.5''$  uncertainty.

place it at  $3600 \pm 250\text{pc}$ . The most recent and accurate center of M71 was found by Goldsbury et al. (2010) who placed the center at  $\alpha = 19\text{h}53\text{m}46.25\text{s}$  and  $\delta = +18^{\circ}46'46.7''$  (J2000) with an error of  $\sim 0.5''$ .

2. DATA REDUCTION AND ANALYSIS

In 2005, we observed M71 with the Near Infrared Imager (NIRI) in conjunction with the ALTAIR adaptive optics system on the Frederick C. Gillett Gemini North Telescope on Mauna Kea (see Figure 1). The observations were carried out in the H ( $1.65\mu\text{m}$ ) and K ( $2.2\mu\text{m}$ ) bands in the core of M71 centered on the star AH 1–83 (Arp & Hartwick 1971). NIRI was set to f/32 to image a field of view of  $22'' \times 22''$  with a pixel scale of  $0.0219''/\text{pixel}$  and a twelve step dither pattern was employed with spacings separated by  $1''$  in both RA and

<sup>1</sup>Department of Physics and Astronomy, University of British Columbia, Vancouver BC V6T 1Z1 Canada: rsamra@phas.ubc.ca, richer@astro.ubc.ca, rgolds@phas.ubc.ca, heyl@phas.ubc.ca, gordonwa@uvic.ca, kwoodley@phas.ubc.ca

<sup>2</sup>Canada-France-Hawaii Corporation, Waimea, HI 96743-8432, United States: karun@cfft.hawaii.edu

TABLE 1  
OBSERVATIONAL LOGS

Date	Filter	Exposure (ksec)	FWHM (")
August 2005	H	15	0.085
August 2005	K	16	0.081
June 2007	H	14	0.083
June 2009	K	23	0.077

Dec. Queue mode observations ensured that for each of our imaging nights, the typical seeing was the best possible at Gemini,  $\leq 0.6''$  in R band. Table 1 contains the observational logs from the three different imaging epochs, all of which used the same instrumental settings aside from the total integration time and filter.

The data were reduced using the GEMINI IRAF package which flat fielded and dark subtracted the raw NIRI data. We used the DAOPHOT II (Stetson 1987) software package to find stars and perform aperture photometry on the individual frames. We then used the DAOMATCH/MASTER tasks to locate the same stars across each of the individual frames, and iteratively rejected stars that were not located on each frame within 1 pixel. Once we had all of the stars on the same coordinate system and the shifts between each of the images due to the telescope’s dither pattern were calculated, a median combined image of the cluster was constructed. This median image was then used to create a deep finding list of 217 stellar-like objects in the NIRI field. ALLFRAME was then run and returned the coordinates for each star in the coordinate system of the median combined image; this package was then used for each of the other imaging epochs to find the coordinates of each stellar object. The error in each star’s position for each epoch was obtained by running ALLFRAME in sets of  $\sim 20$  frames for each individual epoch. This resulted in 7-8 positions for each star for each of the three epochs; the standard deviation of the positions was the resultant error in the position. PMs were then derived by fitting linear time dependent curves for each star’s position as shown in Figure 2.

We then used online data from the ACS Survey of Galactic Globular Clusters in the HST filters F606W and F814W transformed to V and I (Sarajedini et al. 2007; Anderson et al. 2008) to construct a color magnitude diagram (CMD) of our field. The CMD of the HST stars contained in the NIRI field is shown in Figure 3. We used stars which had total PMs less than 0.8 mas/yr (half the PM dispersion of all stars) to define a fiducial main sequence (MS). Our cluster sample consists of all stars within 0.05 magnitudes in color of the MS fiducial, regardless of their measured PM.

A previous PM study of M71 was performed by Cudworth (1985), we used the 358 stars listed in that paper’s table to verify our PMs. We first matched Cudworth’s stars to the ACS photometry to obtain colors for 208 stars. We then performed a color-cut for stars within 0.05 magnitudes of the RGB to define a PM winnowed sample. We then removed all stars from both the NIRI and Cudworth’s winnowed samples which had PM errors greater than  $2\sigma$ . This resulted in 150 cluster members for our NIRI field and 94 stars from Cudworth’s sample. These 94 stars ranged in radial distance between

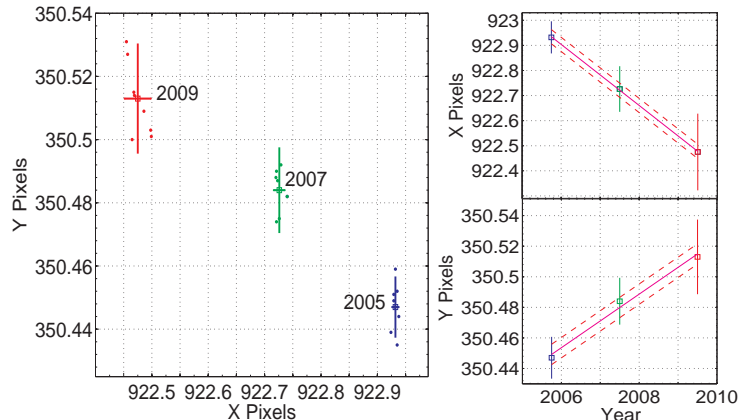


FIG. 2.— *Left:* The relative location of one cluster member across the field in each of the three imaging epochs. The colored dots represent the derived locations from each ALLFRAME run. The error in the final position is determined from the spread in the points for each epoch. *Right:* The X and Y positions of the same star as a function of time. The PM was found from fitting a straight line through those points, the slope of the line multiplied by the NIRI f/32 plate scale gives the PM. The dashed lines represent one-sigma errors.

$6''$ - $150''$  from the cluster center, 5 of which were in our NIRI field for which we did not have PMs due to them being saturated on our frames. Figure 3 has both our NIRI field PMs and Cudworth’s PMs included, the final PM sample we used for this study are the stars in the top-right figure.

### 3. RESULTS

#### 3.1. Proper Motion Distribution

To quantify the velocity dispersion of the cluster, one is tempted to use the standard deviation. However, a single high-velocity interloping star in the sample can skew the standard deviation to arbitrarily large values. Therefore we seek an estimator of the dispersion that is robust to outliers. Rousseeuw & Croux (1993) propose  $Q_n$ , motivated by two of its strengths — its ability to deal with skewness and its efficiency with gaussian distributions. It is defined over all the pairs of stars in the sample,

$$Q_n = a \times \text{first quartile of } (|\mu_i - \mu_j|) : i < j \quad (1)$$

where  $a$  is a constant dependent upon the size of the sample (for large samples  $a \rightarrow 2.2219$ ) and  $\mu_i$  and  $\mu_j$  are observed PMs in a particular direction of pairs of stars in our sample. One further advantage of the  $Q_n$  estimator is that it approximates the standard deviation for distributions which are significantly different from normally distributed distributions such as those close to a uniform distribution. We treat  $Q_n$  as a proxy for the standard deviation for the remaining analysis. For example, we correct for the errors in the observed PMs from the estimated errors to arrive at the PM dispersion:

$$Q_n^2 = Q_{n_o}^2 - \frac{1}{N} \sum \epsilon_{\mu_i}^2 \quad (2)$$

where  $Q_n$  is the error corrected dispersion,  $Q_{n_o}$  is the observed non-error-corrected PM dispersion and  $\epsilon_{\mu_i}$  is the error associated with the PM of each star. The error in the dispersion was calculated by bootstrapping the PMs and their errors 100,000 times and taking the standard deviation of the bootstrapped dispersions. This results

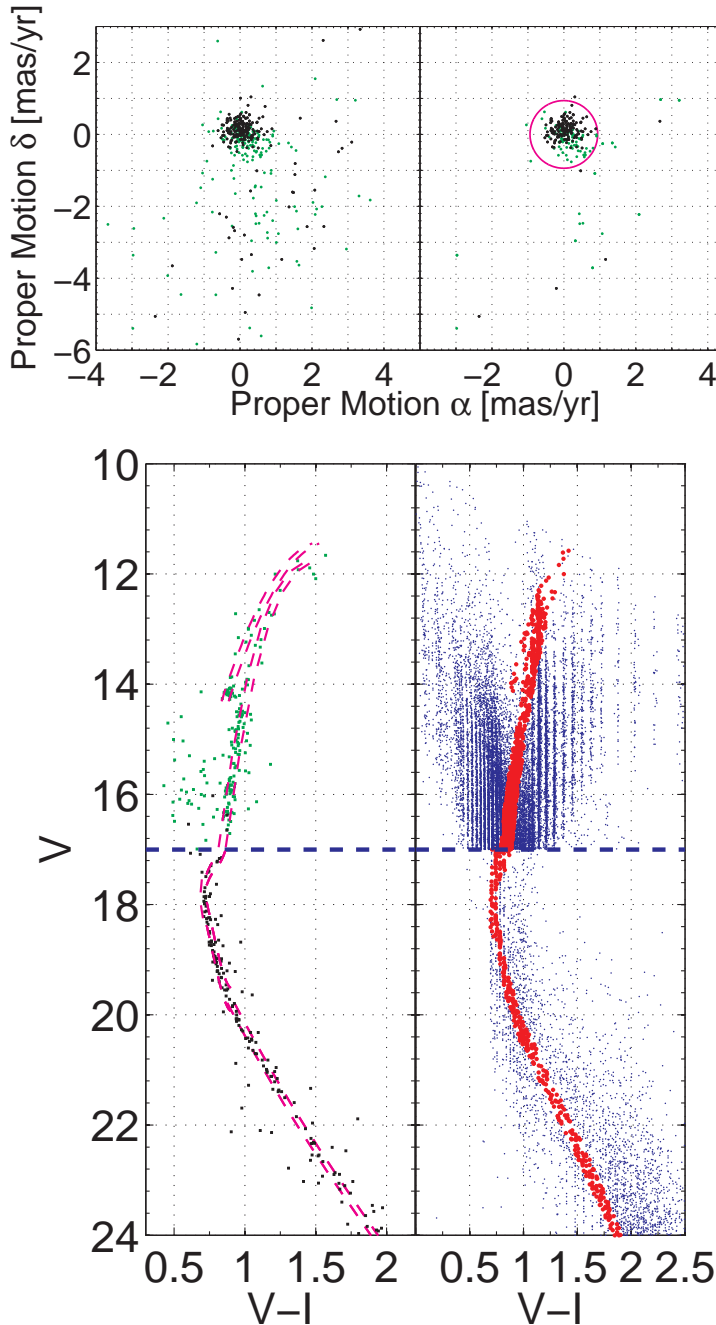


FIG. 3.— *Top Left:* The differential PMs relative to the cluster mean in RA and Dec from the NIRI field (black dots) and all the stars in the field of Cudworth (1985) for which we have ACS photometry (green dots). *Bottom Left:* The CMDs from ACS photometry of both our field and Cudworth (1985). The horizontal blue line represents the cut-off of both studies. We observed stars with  $V > 17$  and Cudworth (1985) only had stars with  $V < 17$ . The curves represent a fiducial MS, likely cluster members are located along this curve. *Top Right:* The PMs of those stars that satisfy the color criterion depicted in the bottom-left panel. The circle depicts an estimate of the escape PM from Gnedin et al. (2002). *Bottom Right:* The CMD of the Besançon models (§ 3.2) for two simulations of the NIRI and Cudworth’s field.

in a one-component core dispersion of  $Q_n = 179 \pm 17 \mu\text{as/yr}$ . Using the familiar standard deviation method to calculate the dispersion we obtain a value of  $\sigma = 185 \pm 18 \mu\text{as/yr}$ , that is after removing stars with PMs greater than the cluster’s escape PM.

We used Cudworth’s stars (see the top right panel of Figure 3) to determine the PM dispersion for stars which had radial distances greater than our NIRI field and were likely cluster members. We found for stars in the inner  $70''$  the dispersion was  $184 \pm 37 \mu\text{as/yr}$ , for stars with distances greater than  $70''$  and up to  $150''$  the dispersion was  $281 \pm 33 \mu\text{as/yr}$ . Results which are similar to the published values from Cudworth (1985).

At the distance of 4 kpc our PM corresponds to a velocity dispersion of  $3.3 \pm 0.4 \text{ km/s}$ , a value greater than the radial velocity dispersion of  $2.0 \text{ km/s}$  obtained by Rastorguev & Samus (1991) and  $2.8 \pm 0.6 \text{ km/s}$  from Peterson & Latham (1986). However those velocity dispersions were calculated for giant stars which were far away from the center of the cluster; a constant dispersion is still within the uncertainties.

### 3.2. High Proper Motion Stars

From the CMD in the bottom left panel of Figure 3, we find 7 stars which have high PMs and survived the winnowing and error cuts. If any of these stars are escaping the cluster, we could determine the cluster’s evaporation timescale purely from observations. However our observed field lies at low Galactic latitude ( $b = -4.56$  degrees), therefore the field may be subject to heavy contamination from the Galactic field as noted by Cudworth (1985). To check for possible interlopers, we used the Besançon models of stellar population synthesis of the Galaxy from Robin et al. (2003). The models depend on the Galactic coordinates, field size, photometric colors, and the extinction. The value for extinction in the direction of M71 was found to be  $0.19 \text{ mag/kpc}$  which was calculated using the reddening constant of  $3.14 \pm 0.10$  from Schultz & Wiemer (1975), the distance, and the reddening from Harris (2010). For a field 100 times the area of our NIRI field, the model yields about 5800 stars, 625 of which lie on our cluster’s main sequence. Therefore we can expect 6 – 7 of the stars in our NIRI field to be interloping field stars (bottom right panel of Figure 3). It is therefore difficult to conclude that we have found any escaping stars.

We also ran a simulation for a field 150 times the size of the ACS field; we find  $\sim 1900$  stars in this simulation which lie on the winnowed CMD for Cudworth’s stars. Scaling this down to the ACS field we expect to find  $\sim 13$  interloping stars. From the PM distribution we find 16 potential escapers, it is once again difficult to conclude we have observed any escaping stars.

### 3.3. Proper Motion Isotropy

Using the PM data, we determine the PM vector of the individual stars in the cluster. We calculated the PM angle with respect to the cluster center for three groups of stars; half of the NIRI field contained stars within  $11''$  the other half were from  $11-22''$ , we also calculated the angles for stars from Cudworth (1985) which we determined to be cluster members. We found that stars in the three different radial distances had PM angles which were consistent with isotropy. We performed a Kuiper test on the data from Figure 4a, which is a test similar to the Kolmogorov-Smirnov test but more sensitive to differences in the wings of the distributions. This test is better suited for distributions which are cyclic in nature

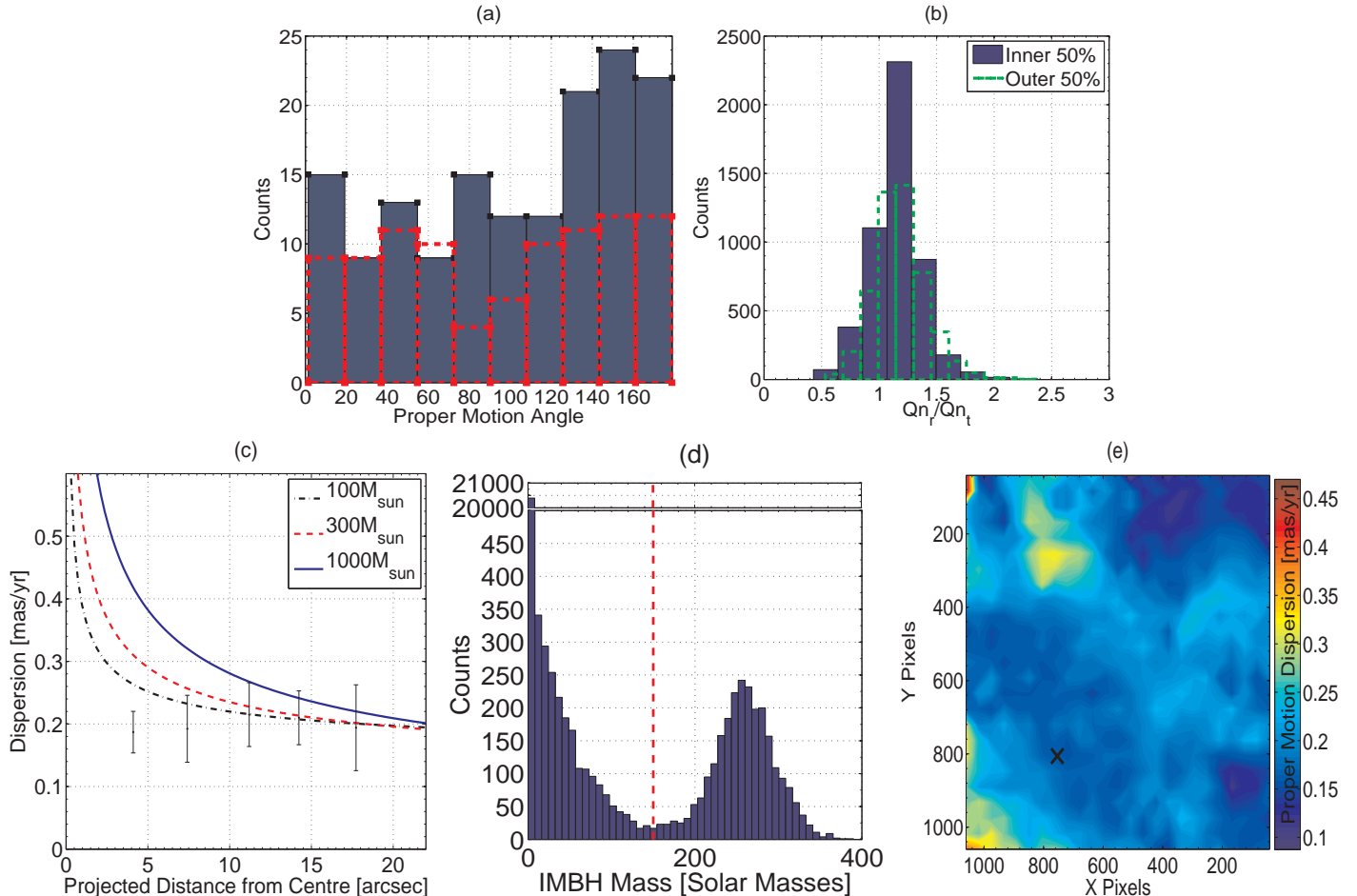


FIG. 4.— *a*: Histogram of the PM angle with respect to the center of the cluster. Blue histograms are for stars in the NIRI field, the dashed red line histogram is for stars from Cudworth (1985). *b*: Histograms for the values  $Q_{n_r}/Q_{n_t}$  resulting from the bootstrap resample of the data. The radial and tangential values of  $Q_n$  are consistent with unity within  $1\sigma$  for all stars. *c*: The observed PM dispersion and three different IMBH models. *d*: The results from bootstrapping the proper motion data 25,000 times, the IMBH mass from each fit is binned here. The leftmost bin from  $0 \leq M_\odot \leq 5$  peaks at 20,500 counts, implying that a very small central IMBH is the preferred fit. The red line represents the 90<sup>th</sup> percentile at  $150M_\odot$ . *e*: A dispersion map of the field, obtained by running a circle with a  $4''$  diameter across the field and calculating the dispersion in each area. Observationally, there are no signs of radial dependence or an increase in dispersion towards the center which is represented by the X.

as in our case. The  $p$ -value, comparing a flat distribution, is 0.17, for stars in the inner  $11''$  and  $p=0.21$  for stars in the outer  $11''$ ; finding no significant difference when compared to a flat isotropic distribution. We have a similar result when we extend our field from the inner  $22''$  up to  $150''$ , we then have a  $p$ -value of 0.14. Figure 4a shows the distributions of PM angles for the NIRI field and from Cudworth.

As we transform coordinates between the multiple epochs, we use cluster stars as the reference points; therefore, any mean motion of the cluster is lost. To characterize the anisotropy of the PMs, we measure the width of the PM distribution in the radial and tangential directions using  $Q_n$ . The measured ratio of the radial to tangential widths  $Q_{n_r}/Q_{n_t}$  is unity for an isotropic distribution. We find the ratio of the two components  $Q_{n_r}/Q_{n_t}$  for three radial distances. For the inner 50% we have  $Q_{n_r}/Q_{n_t} = 1.15 \pm 0.22$  and  $Q_{n_r}/Q_{n_t} = 1.17 \pm 0.23$  for stars for the outer 50% of the NIRI field. If we extend our field up to  $\sim 150''$  we have  $Q_{n_r}/Q_{n_t} = 1.03 \pm 0.13$ . The errors were obtained by bootstrapping our sample of measured PMs, and accounting for errors in the cluster's

center and PMs. Although the results for stars in our NIRI field are above unity and may indicate a stronger radial component in the PMs, both results are still within  $1\sigma$  of unity. Figure 4b shows the distributions of the ratios of the radial and tangential dispersions from our NIRI field.

### 3.4. An Upper Limit to the Mass of any Central IMBH

IMBHs have been suggested to exist in several GCs such as G1 (Gebhardt et al. 2005; Ulvestad et al. 2007), NGC 6388 (Lützgendorf et al. 2011), and Omega Cen (Noyola et al. 2008), however some of the claims are still disputed, notably the claim in Omega Cen (Anderson & van der Marel 2010). Safonova & Shastri (2010) extrapolate the SMBH correlations down to GC masses, determining a linear relation in the velocity dispersion and central black hole mass. Using their relation and our observed velocity dispersion, we obtain an upper limit of a central black hole mass of  $25 M_\odot$  for M71. It is risky, however, to extrapolate correlations between SMBHs down to IMBHs as their formation scenarios might be significantly different. To determine if



we have observed any evidence for a central IMBH in the core of M71, we divide our PM data for stars in the inner  $22''$  into 5 radial bins. Each bin contains 30 stars, we then calculate the observed PM dispersion (Equation 2) and estimate the errors by bootstrapping and calculating the spread in the values of  $Q_n$  (see Figure 4c). The observed PM dispersion is nearly constant throughout the inner  $22''$ .

We have found that the velocity dispersion calculated by Baumgardt et al. (2004) in clusters with a black hole at the center can be modeled simply as a function of the cluster half-light radius for stars which are close to the cluster center. The resulting model contains an  $r^{-1/2}$  Keplerian contribution from the black hole and a constant dispersion from the stars only. To quantify our results we bootstrap the observed PMs and fit them to our model by minimizing the  $\chi^2$  values and accounting for our error in the cluster center. Using these bootstrapped data we find with 90% confidence, that any black hole at the center of M71 must be less massive than  $150d_4^3 M_\odot$ . Where  $d_4$  is the distance to the cluster divided by 4 kpc. From the histogram in Figure 4d the most common result is the one with a very small black hole, where the PM distribution is constant with radius. Near the 90th percentile the value of  $\sigma$  from our model vanishes and the observed PMs obey a Keplerian  $r^{-1/2}$  distribution.

One of the risks with binning data is that it is possible to over- or under-bin and mask or amplify any underlying features or noise. We approach this with two methods. First we run a circular bin across our field and calculate the dispersion in each bin to produce a dispersion map. Figure 4e shows this map and it is clear the changes in dispersion are random fluctuations.

Second, we calculate the average distance from the center,

$$\bar{r} = \Sigma r / N \quad (3)$$

and compare it to the proper motion weighted distance from the center,

$$\bar{r}_{|\mu|} = \frac{\Sigma r |\mu|}{\Sigma |\mu|}. \quad (4)$$

If the PMs are constant as a function of distance from the center, the two values should be equal. However, if PMs are decreasing with increasing radial distance, larger radii get less weight so the value is less. We obtain  $\bar{r} = 11.81'' \pm 0.47''$  and  $\bar{r}_{|\mu|} = 11.50'' \pm 0.83''$ . The PM weighted distance is lower, indicative of higher proper motions at smaller radii, but a radially constant velocity dispersion is completely consistent within the uncertainties.

#### 4. CONCLUSIONS

Using NIRI on the Gemini North Telescope, we have been able to resolve the internal PMs in M71. With a 3.8 year baseline, we have found the PMs for 217 stars, 150 of which are apparent cluster members. Several exhibit high PMs well beyond the escape velocity of the cluster. However, we cannot say with confidence that we are observing any escaping stars because of probable contamination by field stars. The cluster's PM dispersion is found to be  $179 \pm 17 \mu\text{as/yr}$  a result similar to Cudworth (1985). By combining data from Cudworth (1985) we are able to look for signs of anisotropy across the cluster's inner  $150''$ ; however we find that the distributions are consistent with isotropic orbits. Finally, the observed PM dispersion is constant with radius and we are able to put an upper limit to any central dark mass to be less than  $150d_4^3 M_\odot$  at 90% confidence.

This work was supported by NSERC-CRSNG Canada and Gemini proposals GN-2005B-Q38, GN-2007A-Q-59 and GN-2009A-Q-29.

#### REFERENCES

- Anderson, J., Sarajedini, A., Bedin, L. R., et al. 2008, *AJ*, 135, 2055
- Anderson, J., & van der Marel, R. P. 2010, *ApJ*, 710, 1032
- Arp, H. C., & Hartwick, F. D. A. 1971, *ApJ*, 167, 499
- Baumgardt, H., Makino, J., & Ebisuzaki, T. 2004, *ApJ*, 613, 1143
- Baumgardt, H., Makino, J., & Hut, P. 2005, *ApJ*, 620, 238
- Cudworth, K. M. 1985, *AJ*, 90, 65
- Gebhardt, K., Rich, R. M., & Ho, L. C. 2005, *ApJ*, 634, 1093
- Geffert, M., & Maintz, G. 2000, *A&AS*, 144, 227
- Ghez, A. M., Salim, S., Hornstein, S. D., et al. 2005, *ApJ*, 620, 744
- Gnedin, O. Y., Zhao, H., Pringle, J. E., et al. 2002, *ApJ*, 568, L23
- Goldsbury, R., Richer, H. B., Anderson, J., et al. 2010, *AJ*, 140, 1830
- Harris, W. E. 2010, arXiv:1012.3224
- Ibata, R., Bellazzini, M., Chapman, S. C., et al. 2009, *ApJ*, 699, L169
- Lützgendorf, N., Kissler-Patig, M., Noyola, E., et al. 2011, *A&A*, 533, A36
- Maccarone, T. J., Kundu, A., Zepf, S. E., & Rhode, K. L. 2007, *Nature*, 445, 183
- Noyola, E., Gebhardt, K., & Bergmann, M. 2008, *ApJ*, 676, 1008
- Peterson, R. C., & Latham, D. W. 1986, *ApJ*, 305, 645
- Rastorguev, A. S., & Samus, N. N. 1991, *Soviet Astronomy Letters*, 17, 388
- Robin, A. C., Reylé, C., Derrière, S., & Picaud, S. 2003, *A&A*, 409, 523
- Rousseeuw, P.J., & Croux, C. 1993, *Journal of the American Statistical Association*, 88, 1273
- Sarajedini, A., Bedin, L. R., Chaboyer, B., et al. 2007, *AJ*, 133, 1658
- Safonova, M., & Shastri, P. 2010, *Ap&SS*, 325, 47
- Schultz, G. V., & Wiemer, W. 1975, *A&A*, 43, 133
- Stetson, P. B. 1987, *PASP*, 99, 191
- Trenti, M., Ardi, E., Mineshige, S., & Hut, P. 2007, *MNRAS*, 374, 857
- Ulvestad, J. S., Greene, J. E., & Ho, L. C. 2007, *ApJ*, 661, L151